Molecular Mechanism of Ca-ATPase Activation by Halothane in Sarcoplasmic Reticulum†

Brad S. Karon and David D. Thomas*

Department of Biochemistry, University of Minnesota Medical School, Minneapolis, Minnesota 55455

Received February 12, 1993; Revised Manuscript Received May 19, 1993

ABSTRACT: We have studied the molecular mechanism of Ca-ATPase activation in sarcoplasmic reticulum (SR) by the volatile anesthetic halothane. Using time-resolved phosphorescence anisotropy, we determined the rotational correlation times and mole fractions of different oligomeric states of the enzyme, as a function of halothane and temperature. Lipid fluidity was measured independently, using EPR of spin-labeled lipids. At 4 and 7 °C, the principal effects of halothane were to increase the activity of the Ca-ATPase and to promote the formation of monomers and dimers of the enzyme from larger aggregates. At higher temperatures (up to 25 °C), halothane activated the enzyme, but to a lesser extent than observed at lower temperatures. While the functional effects of halothane were temperature dependent, the effects of halothane on lipid fluidity and protein aggregation state were similar at all temperatures tested. We conclude that at low temperatures Ca-ATPase activity is dominated by aggregation state, so halothane activates the enzyme primarily by promoting the formation of monomers and dimers of the enzyme from larger aggregates. At higher temperatures, the activity of the enzyme is dominated by lipid fluidity, so halothane activates the enzyme by increasing the lipid fluidity. The physical mechanism of Ca-ATPase activation, dominated by aggregation state at low temperature and lipid fluidity at higher temperature, provides an explanation for the break in the Arrhenius plot of Ca-ATPase activity (in the absence of halothane) at approximately 20 °C.

To understand the mechanism of anesthetic action, many studies have been conducted on the effect of halothane, a general anesthetic, on the function and physical properties of biological membranes. These studies have focused on two areas: the effects of general anesthetics on the physical properties of membranes, such as lipid fluidity, and the direct interaction of anesthetics with membrane proteins. Because the effect of halothane and other general anesthetics on lipid fluidity is minimal at clinical levels, recent investigations have focused more on the direct interaction of anesthetics with proteins and the ability of anesthetics to alter other physical properties of biological membranes (Akeson & Deamer, 1991; Franks & Lieb, 1991). The physical properties being studied include boundary lipid effects, local phase changes in the membrane, and protein–protein interactions (Bigelow et al., 1987; Taraschi et al., 1991; Trudell, 1991; Watts, 1991). The study of anesthetic effects on the physical properties of biological membranes may not only provide insight into the molecular action of general anesthetics but also shed light on the physical rules that govern membrane proteins.

Sarcoplasmic reticulum (SR)[1] membrane, from rabbit skeletal muscle, offers several advantages as a model system for studying the physical effects of halothane on biological membranes. First, the effects of many physical parameters, such as lipid fluidity, protein rotational mobility, and protein aggregation state, on SR function have been well documented (Squier et al., 1988a,b; Birmachu & Thomas, 1990). Second, changes in lipid physical parameters, such as SR lipid fluidity and boundary lipid mobility, have been correlated with changes in protein physical parameters such as oligomeric state and rotational mobility of the Ca-ATPase (Bigelow & Thomas, 1987; Birmachu & Thomas, 1990). Third, the techniques for measuring lipid fluidity, protein mobility (which includes both rotational mobility and oligomeric state), and SR function (as measured by Ca-ATPase activity) are easily applied to the study of anesthetics. Fourth, the effects of other physical perturbants, such as temperature, ether, alcohols, and melittin, on lipid–protein interactions and Ca-ATPase activity have been studied (Bigelow et al., 1986; Bigleow & Thomas, 1987; Lopes & Louro, 1991; Mahaney & Thomas, 1991; Mahaney et al., 1992). By using these physical perturbants, an understanding of how the various physical parameters are related to each other and SR function is beginning to emerge. Thus, the motivation for studying the effect of halothane on SR is 2-fold: to understand how halothane interacts with biological membranes and to understand how biological membranes, in this case SR, are regulated by their physical properties.

Previous reports on the effects of halothane on SR Ca-ATPase activity have reached a number of different conclusions. Some investigators have reported an increase in Ca-ATPase activity at clinically relevant levels of halothane (Nelson & Sweo, 1988; Blanck et al., 1992; Louis et al., 1992), while others have reported no effect on Ca-ATPase activity at these levels (Diamond & Berman, 1980; Rock et al., 1990). At higher levels, halothane has been reported to inhibit Ca-ATPase activity (Diamond & Berman, 1980; Nelson & Sweo, 1988; Louis et al., 1992). These apparent discrepancies can only be fully resolved by a more detailed investigation into the physical mechanism of halothane's effect on SR function.

In the present study, changes in Ca-ATPase activity induced by halothane were correlated with changes in SR lipid fluidity as measured by EPR and in protein rotational mobility and oligomeric state as measured by time-resolved phosphorescence anisotropy (TPA). By using three different techniques, each

† This work was supported by NIH Grant GM27906 to D.D.T. B.S.K. was supported by a predoctoral training grant from NIH.

* Author to whom correspondence should be addressed.

[1] Abbreviations: SR, sarcoplasmic reticulum; EPR, electron paramagnetic resonance; ATP, adenosine triphosphate; MOPS, 3-(*N*-morpholino)propanesulfonic acid; DMF, *N*,*N*-dimethylformamide; NADH, β-nicotinamide adenine dinucleotide, reduced form.

0006-2960/93/0432-7503$04.00/0

one most sensitive to the parameters being measured, we were able to correlate Ca-ATPase activity, lipid fluidity, and protein mobility. Using this approach, we have investigated the molecular mechanism of halothane action on the Ca-ATPase, and the results provide further insight into the roles of lipid fluidity and protein mobility in regulating SR function.

MATERIALS AND METHODS

Reagents and Solutions. Erythrosin 5-isothiocyanate (ERITC) was obtained from Molecular Probes, Inc. (Eugene, OR) and stored in DMF at −70 °C. ATP, catalase, glucose, and glucose oxidase type IX were obtained from Sigma. Halothane (99%) and spin labels were obtained from Aldrich. All experiments were carried out in a standard buffer containing 60 mM KCl, 6 mM $MgCl_2$, 0.1 mM $CaCl_2$, and 20 mM MOPS (pH 7.0).

Preparations and Assays. SR vesicles were prepared from the fast twitch skeletal muscle of New Zealand white rabbits (Fernandez et al., 1980). The vesicles were purified on a discontinuous sucrose gradient (Birmachu et al., 1989) to remove heavy SR vesicles (junctional SR containing calcium release proteins). All preparation was done at 4 °C. SR pellets were resuspended in 0.3 M sucrose and 20 mM MOPS (pH 7.0), rapidly frozen in 4-mg aliquots, and stored in liquid nitrogen until use. The ATP hydrolysis of the SR vesicles was fully coupled to calcium transport (Squier & Thomas, 1989). SR lipids were extracted by a modification (Hidalgo et al., 1976) of the method of Folch et al. (1957), using nitrogen-saturated solvents to prevent oxidation. The lipids were stored in chloroform–methanol (2:1) under nitrogen at −20 °C.

The SR activity was measured using an enzyme-linked, continuous ATPase assay, in the standard buffer with the addition of 5–50 μg/mL SR, 2 mM phosphoenolpyruvate, 0.24 mM NADH, 120 IU of pyruvate kinase, and 120 IU of lactate dehydrogenase. ATP (200 μM) was added to start the assay, and the absorbance of NADH was monitored at 340 nm to determine the rate of ATP hydrolysis. Activity measurements in the presence of ionophore were done by adding 1 μg/mL of the ionophore, A23187, to the SR prior to the start of the assay. Addition of the ionophore allows the Ca-ATPase activity to be measured in the absence of a Ca gradient, so that any vesicle leakiness produced by the addition of halothane will not affect the actvity measured (Bigelow & Thomas, 1987). The activity measured in the presence of ionophore gives a maximal Ca-ATPase activity, since the enzyme does not have to work against a concentration gradient. Halothane, 30–50% v/v in DMF, was added with a Hamilton syringe, by injecting a small amount (less than 1% of the total sample volume) of halothane through a septum in the cuvette. The samples were allowed to incubate for 5 min, using a stir bar to allow for mixing. The volumes of SR and halothane used were adjusted to minimize the vapor space above the SR, so that the amount of halothane that partitioned into the vapor phase was negligible. The final volume of DMF added, up to 1% v/v, did not affect Ca-ATPase activity.

Determination of Halothane Concentration. The concentration of halothane in solution used for the activity, TPA, and EPR experiments was verified by UV spectroscopy of halothane in heptane, according to the method of Blanck et al. (1980). The concentration of halothane, expressed as moles per liter present in the lipid bilayer, was calculated using a partition coefficient of 45 (Eckenhoff & Shuman, 1991), assuming that the concentration of halothane in the membrane is equal to the concentration in solution times the partition coefficient. This should be true so long as the lipid fraction of the sample is negligible compared to the solution fraction, which is the case in TPA and activity experiments. For EPR experiments, the membrane concentration was estimated using the partition coefficient and the fraction of lipid in the sample. All halothane concentrations are expressed as concentration in the membrane ($[halothane]_m$). The amount of halothane necessary for general anesthesia has been estimated to be between 0.03 and 0.05 mol of halothane/mol of lipid in the bilayer (Taraschi et al., 1991). Thus, clinical levels of anesthetic are approximately 30–50 mM in the bilayer, roughly the same concentration as the lowest level used in the activity and optical experiments.

Optical Spectroscopy. TPA decays were obtained as described previously (Ludescher & Thomas, 1988). The phosphorescence anisotropy decay $r(t)$ is given by

$$r(t) = \frac{I(t)_{vv} - GI(t)_{vh}}{I(t)_{vv} + G2I(t)_{vh}}$$

where $I(t)_{vv}$ and $I(t)_{vh}$ are obtained by signal-averaging the time-dependent phosphorescence decays following 2000 laser pulses, with a single detector and a polarizer that alternates between the vertical $[I(t)_{vv}]$ and horizontal $[I(t)_{vh}]$ positions every 2000 pulses. The laser repetition rate was 200 Hz, so a typical $r(t)$ acquisition required 4–8 min to complete 10 or 20 loops, or cycles, of 4000 laser pulses each (2000 in each orientation). G is an instrumental correction factor, determined by measuring the anisotropy of free dye in solution under experimental conditions.

Optical Labeling and Sample Preparation. For phosphorescence experiments, the Ca-ATPase was specifically labeled at lysine 515 with ERITC as described previously (Birmachu & Thomas, 1990). Oxygen was enzymatically removed from the TPA samples with 100 μg/mL glucose oxidase, 15 μg/mL catalase, and 5 mg/mL glucose, according to the method of Eads et al. (1984). Deoxygenation was carried out in a sealed cuvette containing 0.2 to 0.3 mg/mL SR protein for 15–25 min prior to phosphorescence data collection. Halothane, 30–50% v/v in DMF, was added to the SR in a manner analogous to the technique used for activity measurements. The final concentration of DMF, up to 0.5% v/v, did not affect the anisotropy decay of SR.

Data Analysis. TPA decays were analyzed as reported previously (Birmachu & Thomas, 1990), using a nonlinear least-squares fit to a sum of exponentials. Before fitting, four intensity files $[I(t)_{vv}$ and $I(t)_{vh}]$ from experiments performed under the same conditions were added, allowing an averaged anisotropy decay to be calculated. Averaged anisotropy decays were fit to a sum of n exponentials plus a constant

$$r(t)/r_0 = \sum_{i=1}^{n} A_i \exp(-t/\phi_i) + A_\infty$$

where ϕ_i are rotational correlation times, A_i are the normalized amplitudes (r_i/r_0), A_∞ is the normalized residual anisotropy (r_∞/r_0), and r_0 is the initial anisotropy $[r(0) = r_0 = \sum r_i + r_\infty]$. The goodness of fit for the anisotropy decays was evaluated by comparing χ^2 values for the multiexponential fits and by comparing plots of the residuals (the difference between the measured and the calculated values). The averaged anisotropy decays were nearly identical to anisotropy decays calculated from individual intensity files but had several advantages. Both systematic noise and random noise in data acquisition were reduced by using averaged anisotropy decays, and the residuals from averaged fits were smaller than those from individual fits, with little change in the χ^2 values. In addition,

the parameters obtained from fitting averaged anisotropy decays showed less scatter when plotted against $[halothane]_m$ than those obtained from fitting individual decays. Phosphorescence lifetimes were analyzed by fitting the total intensity ($I_{vv} + 2I_{vh}$) in a manner analogous to the anisotropy decay fitting. Halothane, at the concentrations used in TPA experiments, did not have significant effects on phosphorescence lifetimes. At higher concentrations, however, halothane quenched the phosphorescence of ERITC-labeled SR.

The Saffman–Delbrück equation describes the rotational diffusion coefficient for uniaxial rotation of a cylindrical membrane protein expressed as a function of membrane lipid viscosity (η), temperature (T), and effective radius (a) of the portion of the protein in the bilayer (Saffman & Delbrück, 1975)

$$D_m = kT/(4\pi a^2 h\eta) \quad (1)$$

where h is the thickness of the hydrocarbon phase of the lipid bilayer. Thus, the rotational mobility ($1/\phi$, inversely proportional to the rotational correlation time) should be proportional to the lipid fluidity (T/η; Squier et al., 1988b) and inversely proportional to the intramembrane area (πa^2) of the rotating protein. Therefore, increasing lipid fluidity or decreasing protein size (formation of smaller oligomers) should result in increased rotational mobility. This theory relating protein size and lipid fluidity to protein rotational mobility is supported by previous studies on the Ca-ATPase, as measured by either ST-EPR (Squier et al., 1988a,b) or phosphorescence anisotropy (Birmachu & Thomas, 1990). Using this theory, Birmachu and Thomas (1990) showed that correlation times obtained by fitting TPA decays can be used to determine the sizes of Ca-ATPase oligomers, and normalized amplitudes can be used to determine the mole fractions of oligomers present in SR.

Spin Labeling and Sample Preparation. Hydrocarbon chain rotational mobility was measured with stearic acid spin labels (designated *N*-SASL), which are *N*-oxyl-4′,4′-dimethyloxazolidine derivatives of stearic acid. Incorporation of 5-SASL into SR lipid was accomplished by adding the spin label to extracted lipids in a chloroform–methanol (2:1 v/v) mixture prior to drying with nitrogen. The spin-labeled lipid was lyophilized for at least 16 h and then resuspended in experimental buffer to a concentration of 40–50 mM. The labeled lipid suspension was transferred to a glass capillary that had been sealed at one end. Halothane, 10–20% in DMF, was injected into the lipid suspension using a Hamilton syringe, and the capillary was promptly sealed with the closed end of a larger capillary that had previously been coated with silicone grease to ensure a good seal. The volumes of lipid and halothane solution added to the capillary were adjusted to minimize vapor space above the lipid sample, and a small glass bead placed in the capillary prior to halothane addition allowed for mixing of the halothane and lipid. The amount of DMF added to the lipid sample (up to 2% v/v) did not produce any changes in the order parameter measured in the absence of halothane.

EPR Spectroscopy. EPR spectra were acquired using a Bruker ESP-300 spectrometer, equipped with a Bruker ER4102 cavity, and digitized with the spectrometer's built-in microcomputer using Bruker OS-9-compatible ESP 1620 spectral acquisition software. Spectra were downloaded to an IBM-compatible microcomputer and analyzed using software developed in our laboratory by R. L. H. Bennett. Conventional (V_1) EPR was used to detect submicrosecond motions of the lipid spin labels. V_1 spectra were obtained using 100-kHz field modulation (with a peak-to-peak modulation amplitude of 2 G), with microwave field intensities (H_1) of 0.14 G. Sample temperature was controlled to within 0.5 °C with a Bruker ER 4111 variable-temperature controller and monitored with a Sensortek Bat-21 digital thermometer using an IT-21 thermocouple probe inserted into the top of the sample capillary, so that it did not interfere with spectral acquisition.

EPR Spectral Analysis. Fatty acid spin label spectra were analyzed by measuring the inner ($2T'_\perp$) and outer ($2T'_\parallel$) spectral splittings. The effective order parameter (S) was calculated from the splittings according to the method of Gaffney (1976)

$$S = \frac{T'_\parallel - (T'_\perp - C)}{T'_\parallel + 2(T'_\perp + C)} \times 1.66$$

where $C = 1.4 - 0.053(T'_\parallel - T'_\perp)$ and $2T'_\perp$ and $2T'_\parallel$ are the measured splittings between the inner and outer extrema resolved in the EPR spectrum.

To facilitate direct comparisons between halothane-induced changes in SR lipid hydrocarbon chain dynamics and protein rotational mobility, the effective lipid fluidity parameter, T/η, was used (Squier et al., 1988b)

$$S = -0.42[\log(T/\eta)] + 0.56$$

where S is the apparent order parameter measured from the V_1 spectrum of 5-SASL and η is the effective lipid viscosity. This is consistent with conventional, qualitative definitions of lipid fluidity, since (a) an increase in the fluidity (T/η) corresponds to a decrease in S, i.e., an increase in the amplitude of hydrocarbon chain reorientation, and (b) it yields a higher fluidity value (more motional freedom) near the center of the bilayer than near the headgroup region (Squier et al., 1988b). However, it differs from conventional fluidity expressions, because (a) it is based on an empirical calibration in which EPR experiments were performed on solvents of known viscosity η, (b) the resulting measurement of lipid fluidity (T/η) agrees quantitatively with the hydrodynamic theory of Saffman and Delbrück (1975), and (c) the observed lipid fluidity varies as expected with the change in rotational correlation times of proteins measured by TPA (Birmachu & Thomas, 1990).

RESULTS

Effect of Halothane on Ca-ATPase Activity at 4 °C. The effect of halothane on SR Ca-ATPase activity, both in the absence and presence of the ionophore, A23187, was measured at 4 °C using an enzyme-linked assay. Figure 1 demonstrates the effect of halothane, from 0 to 314 mM in the membrane, on Ca-ATPase activity. Halothane stimulated Ca-ATPase activity at all concentrations tested, both in the presence and in the absence of ionophore. The extent of activation by halothane in the absence of ionophore was slightly greater than that measured in the presence of ionophore. This indicates that vesicle leakiness probably contributes to the activation of the enzyme by halothane in the absence of ionophore. The maximal Ca-ATPase activity, that measured in the presence of ionophore, was approximately doubled by 314 mM halothane.

Effect of Halothane and Temperature on SR Lipid Fluidity. To determine the effect of halothane on SR lipid fluidity, we used EPR spectroscopy to determine the fluidity of protein-free, aqueous dispersions of extracted SR lipid, as described under Materials and Methods. The lipid dispersions were

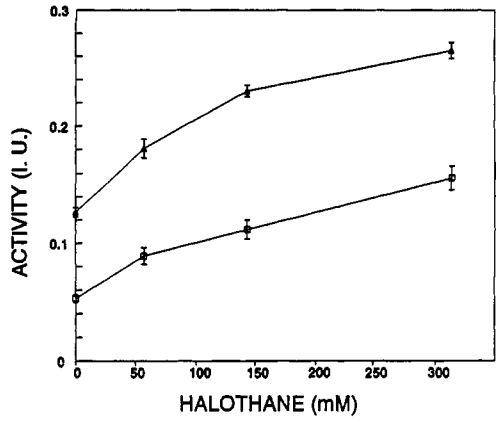

FIGURE 1: Effect of halothane (millimolar in the membrane) on SR Ca-ATPase activity at 4 °C, in units of micromoles of ATP hydrolyzed per milligram of protein per minute (IU), as measured by an enzyme-linked, continuous ATPase assay, described under Materials and Methods. Activity is measured in the absence (□) and presence (▲) of 1 μg/mL of ionophore, A23187. Each point represents the average of four experiments ± the standard error of the mean.

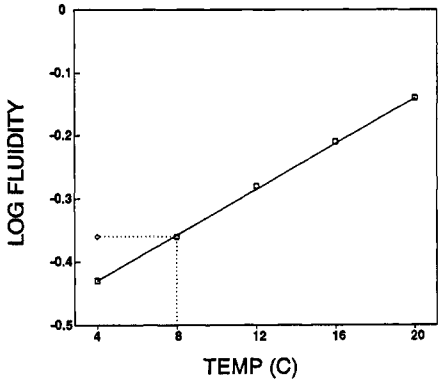

FIGURE 2: Effect of temperature and halothane on SR lipid fluidity (T/η), determined from order parameters as described under Materials and Methods. The open squares (□) represent the fluidity of SR lipid determined at 4, 8, 12, 16, and 20 °C. The circle (○) represents the fluidity of SR lipid at 4 °C with 311 mM halothane added, showing that 311 mM halothane (in the membrane) has the same effect on lipid fluidity as raising the temperature of control SR lipid by 4 °C.

spin-labeled with a stearic acid spin label at the 5-carbon position, which is sensitive to bilayer fluidity near the headgroup of the bilayer. At 4 °C, a halothane concentration of 311 mM increased the SR lipid fluidity by 19%, from 0.37 to 0.44. In comparison, the activity of the Ca-ATPase was doubled by the same concentration of halothane.

The effect of temperature on control SR lipid (SR lipid without halothane) was also measured to calculate an "effective temperature change" of halothane on SR lipid fluidity. Expressing the effect of a physical perturbant on SR properties in terms of a temperature change provides a means to compare changes in different physical parameters due to the perturbant. This has been done to compare the effects of ether on SR Ca-ATPase activity, lipid fluidity, and protein mobility (Bigelow & Thomas, 1987). As shown in Figure 2, the addition of 311 mM halothane to SR lipid at 4 °C increases bilayer fluidity by 19%, the same effect produced by raising the temperature from 4 to 8 °C in the absence of halothane. Thus, 311 mM halothane in the membrane produces a 4 °C effective temperature increase in lipid fluidity.

Effect of Halothane on Protein Rotational Dynamics at 4 °C. TPA experiments were performed to determine the effect of halothane on SR protein rotational mobility. The TPA

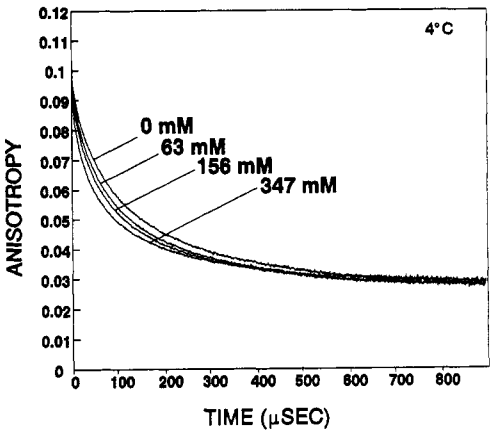

FIGURE 3: TPA decays of ERITC-labeled SR at 4 °C in standard buffer with the addition of various levels of halothane. TPA decays at 0, 63, 156, and 347 mM halothane (in the membrane) are shown, with each addition of halothane resulting in a relatively faster anisotropy decay.

decays of ERITC-labeled SR at 4 °C demonstrated a pronounced effect of halothane on the rotational dynamics of the Ca-ATPase. Figure 3 shows the anisotropy decays resulting from the addition of progressively greater amounts of halothane. Qualitatively, halothane increases the mobility of the Ca-ATPase, without significantly changing A_∞. There are two possible mechanisms for this action, which are not mutually exclusive: halothane either (a) increases the rotational mobility of all aggregates of the Ca-ATPase (in which case the correlation times should decrease) or (b) changes the average aggregate size to favor smaller, more rapidly rotating aggregates at the expense of larger ones (in which case the amplitudes, which represent the fraction of enzyme present in a given oligomeric state, should change).

To determine the effects of halothane on the aggregation state (amplitudes) and rotational correlation times of the Ca-ATPase in SR, the anisotropy decays were fit as described under Materials and Methods. The decays were best fit to a sum of three exponentials plus a residual anisotropy (A_∞). These three components have previously been observed and are interpreted to represent the rotational motion of monomers (A_1), dimers (A_2), and larger aggregates (A_3) of the Ca-ATPase, although no definite assignment of amplitudes to oligomeric states can be made (Birmachu & Thomas, 1990). The normalized amplitudes, rotational correlation times, and A_∞ values are given in Table I.

The correlation times, ϕ_1, ϕ_2, and ϕ_3, each decreased upon the addition of halothane up to 347 mM. If the increased rates of rotational motion were due to an increase in lipid fluidity, as predicted by the Saffman–Delbrück equation (eq 1), then an Arrhenius plot should show a linear relationship between rotational mobility ($1/\phi$) and $[\text{halothane}]_m$, as was previousy observed for the relationship of Ca-ATPase rotational mobility and temperature (Birmachu & Thomas, 1990). Figure 4 demonstrates that the log of the rotational mobility of all Ca-ATPase aggregates decreased linearly with $[\text{halothane}]_m$. By comparing the change in $\log(1/\phi)$ vs $[\text{halothane}]_m$ with the change in $\log(1/\phi)$ vs temperature obtained by Birmachu and Thomas (1990), the effective temperature change induced by 347 mM halothane was determined to be approximately 4 °C. A similar concentration of halothane (311 mM) also produced a 4 °C effective temperature change in lipid fluidity. Thus, the increased rates of rotational motion seen upon the addition of halothane most likely result from the increase in lipid fluidity induced by halothane.

Table I: Anisotropy Decay Parameters for SR at 4 °C[a]

sample	A_1	ϕ_1	A_2	ϕ_2	A_3	ϕ_3	A_∞
control	0.07 ± 0.01	9 ± 1	0.28 ± 0.01	57 ± 3	0.37 ± 0.02	257 ± 8	0.27 ± 0.01
63 mM	0.09 ± 0.01	8 ± 1	0.29 ± 0.01	52 ± 1	0.34 ± 0.01	245 ± 2	0.27 ± 0.01
156 mM	0.10 ± 0.01	8 ± 1	0.30 ± 0.01	49 ± 3	0.33 ± 0.01	245 ± 22	0.28 ± 0.01
347 mM	0.12 ± 0.01	6 ± 1	0.28 ± 0.01	39 ± 1	0.30 ± 0.01	217 ± 6	0.30 ± 0.01

[a] TPA parameters were determined by fitting the averaged anisotropy decays of SR at 4 °C with the addition of 0, 63, 156, and 347 mM halothane in the membrane. As described under Materials and Methods, each anisotropy decay is calculated by summing four intensity files [$I(t)_w$ and $I(t)_{vh}$] from experiments performed under the same conditions. These anisotropy decays are then fit, by nonlinear least-squares analysis, to obtain values for the correlation times (ϕ), normalized amplitudes ($A_i = r_i/r_0$), and A_∞ (r_∞/r_0). The values of r_0 were 0.100 ± 0.001, 0.099 ± 0.001, 0.097 ± 0.001, and 0.096 ± 0.001 for the control and 63, 156, and 347 mM fits, respectively. To estimate the error in the values, each intensity file used to obtain an averaged anisotropy decay was fit individually (i.e., for every averaged parameter, four individual parameters were determined). The correlation times, amplitudes, and A_∞ values obtained in this manner were used to calculate the standard error of the mean for each averaged value. Numbers in the table represent the averaged value ± the standard error of the mean (n = 4).

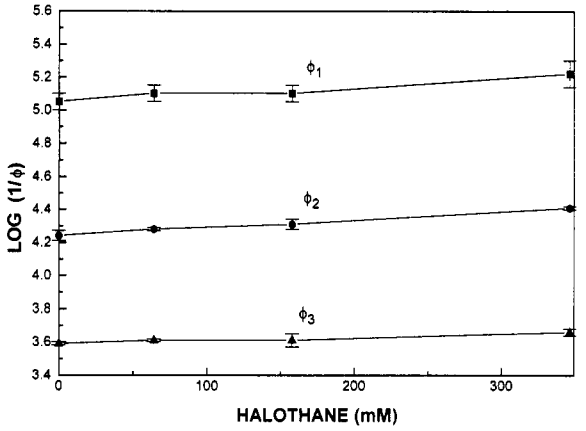

FIGURE 4: Effect of halothane on the rotational correlation times, ϕ_1 (■), ϕ_2 (●), and ϕ_3 (▲), determined by fitting the anisotropy decays presented in Figure 3, as described under Materials and Methods. The correlation coefficients for the lines representing ϕ_1, ϕ_2, and ϕ_3, are 0.92, 0.99, and 0.93, respectively, indicating that the data fit a straight line. Each point represents the average of four experiments ± the standard error of the mean.

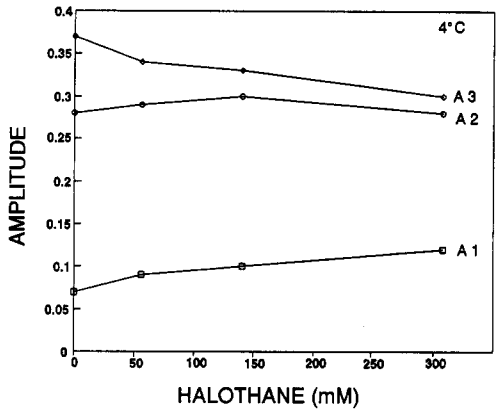

FIGURE 5: Effect of halothane on the normalized amplitudes, A_1 (□), A_2 (○), and A_3 (◇), determined by fitting the anisotropy decays presented in Figure 3, as described under Materials and Methods. Each point represents the average of four experiments; the values and standard errors of the mean are given in Table I.

The amplitudes obtained from fitting the anisotropy decays, however, did not vary with halothane concentration in the same manner as the correlation times (Figure 5). Birmachu and Thomas (1990) previously observed a linear increase in A_1 and A_2, and a linear decrease in A_3, as the temperature was raised from 4 to 20 °C. However, in the current study, addition of halothane at 4 °C resulted in an increase in A_1, an initial increase then decrease upon further addition of halothane for A_2, and a decrease in A_3. By comparing the maximum changes in amplitudes upon the addition of 347 mM halothane with

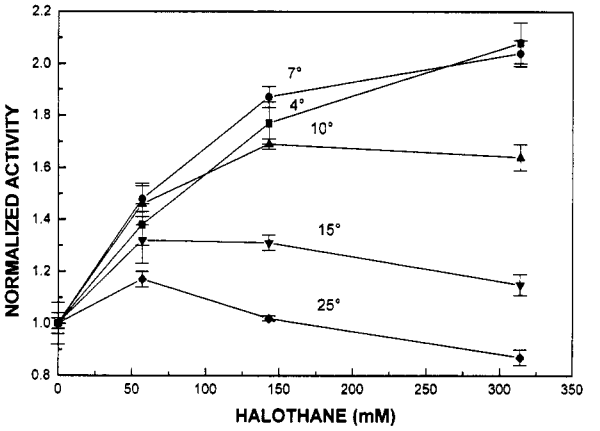

FIGURE 6: Effect of halothane (millimolar in the membrane) on SR Ca-ATPase activity, in units of micromoles of ATP hydrolyzed per milligram of protein per minute (IU), in the presence of 1 μg/mL of the ionophore, A23187, at various temperatures; as measured by an enzyme-linked, continuous ATPase assay, described under Materials and Methods. Activity, normalized to the control (no halothane added) at each temperature, is measured at 4 (■), 7 (●), 10 (▲), 15 (▼), and 25 °C (♦). Each point represents the average of two to four experiments ± the standard error of the mean.

the rates of change of amplitudes with increasing temperature from Birmachu and Thomas (1990), we calculated the effective temperature changes of the amplitudes. The increase in A_1 corresponds to an 8 °C effective temperature increase, while the decrease in A_3 corresponds to a 4 °C effective temperature increase. The halothane-induced change in A_2 cannot be correlated with a temperature change, because A_2 changes in a biphasic manner with increasing amounts of halothane, whereas this is not seen with increasing temperature.

Effect of Halothane on SR at Higher Temperatures. The effect of temperature on the activation of the Ca-ATPase by halothane was examined by measuring the enzyme activity, in the presence of ionophore, at 4, 7, 10, 15, and 25 °C, as described previously. The activities, normalized to the control activity at each temperature, are shown in Figure 6. At 4 and 7 °C, halothane up to 314 mM in the membrane increased the activity of the enzyme, with the maximum activation being approximately double the activity of the control. At higher temperatures, however, halothane activated the enzyme at lower concentrations, but this activation was reversed at higher concentrations of halothane. At 25 °C, the maximum activation was only 17% greater than the control activity, and halothane at 314 mM actually inhibited the enzyme relative to the control.

To determine whether halothane had temperature-dependent effects on lipid fluidity or protein mobility, EPR and TPA experiments were performed at 25 °C. Halothane increased lipid fluidity by the same fraction at both 4 and 25

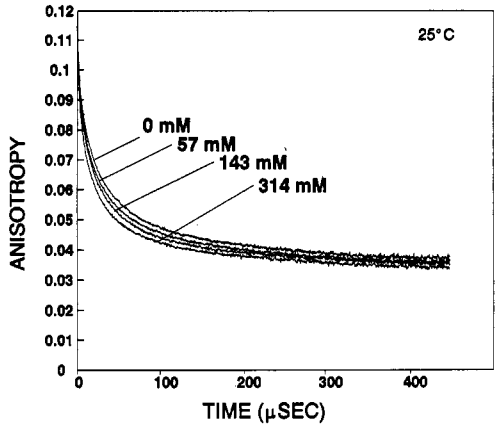

FIGURE 7: TPA decays of ERITC-labeled SR at 25 °C in standard buffer with the addition of various levels of halothane. TPA decays at 0, 57, 143, and 314 mM halothane (in the membrane) are shown, with each addition of halothane resulting in a relatively faster anisotropy decay.

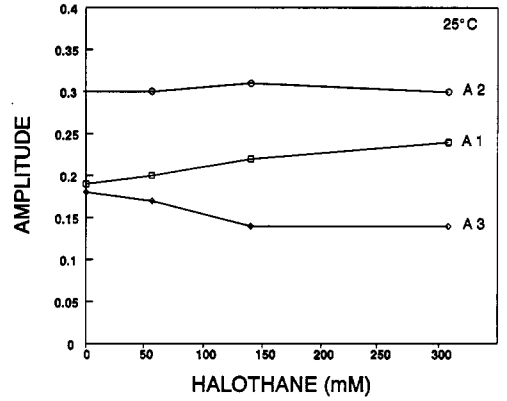

FIGURE 8: Effect of halothane on the normalized amplitudes A_1 (□), A_2 (○), and A_3 (◇), determined by fitting the anisotropy decays presented in Figure 7, as described under Materials and Methods. Each point represents the average of four experiments; the standard error of the mean is less than or equal to 0.01 for all points.

°C, while the effect of halothane on protein rotational motion was significantly different at the two temperatures.

Figure 7 shows the anisotropy decays of SR in the presence of increasing $[halothane]_m$ at 25 °C. The decays were fit according to the same procedure used to analyze the data at 4 °C, and the normalized amplitudes of SR protein aggregates are plotted in Figure 8. A_2 is now the dominant amplitude and changes little with the addition of halothane. A_1 increases at the expense of A_3 with increasing levels of halothane, as was observed at 4 °C. However, the relative decrease in A_3 is now smaller, corresponding to an effective temperature change of only 2 °C. The increase in A_1 is similar to the change observed at 4 °C, again corresponding to an effective temperature change of 8 °C. The value of A_∞ (not shown) did not change with the addition of halothane at 25 °C.

DISCUSSION

Effect of Halothane on Ca-ATPase Activity. Our study of halothane's effect on Ca-ATPase activity (Figure 1) may help to explain the discrepancies in previous papers. Previous studies at temperatures above 20 °C have shown that halothane activates the Ca-ATPase at clinical concentrations, and this activation is reversed at higher concentrations of the anesthetic (Nelson & Sweo, 1988; Louis et al., 1992). However, many of these studies, as well as some reports that showed no activation of the Ca-ATPase, were done by using Ca uptake as a means of measuring activity (Nelson & Sweo, 1988; Louis et al., 1992). Because our activity assays, in agreement with previous studies (Rock et al., 1990; Blanck et al., 1992), indicate that halothane may induce leakiness in SR vesicles, Ca uptake data may be misleading as an indicator of activity in the presence of halothane.

The temperature dependence of the Ca-ATPase activation by halothane (Figure 6) demands further explanation. Given that the physical effects of halothane on SR are similar between 4 and 25 °C, there are several possibilities that might explain the temperature-dependent nature of halothane action. At higher temperature, there could be some irreversible loss of enzyme activity, such as protein denaturation, or perhaps the lipid fluidity exceeds some optimum value. A third possibility is that the aggregation state of the enzyme becomes less favorable when halothane is added at higher temperatures.

To rule out the first possibility, that adding halothane at higher temperatures results in an irreversible loss of enzyme activity, we added halothane to SR at 25 °C and then measured enzyme activity at 7 °C. The enzyme activity measured in this manner was the same as the activity measured when halothane was added at 7 °C. Therefore, adding halothane to SR at 25 °C does not irreversibly inactivate the ATPase. To explore the other two possibilites, that halothane at higher temperatures may result in either a hyperfluid lipid environment or an unfavorable aggregation state, we must first examine the effect of temperature alone on fluidity, aggregation state, and enzyme activity.

Effect of Temperature on SR. To examine the effect of temperature on the rotational dynamics of the Ca-ATPase, it is desirable to distinguish the effects of temperature on membrane fluidity from the effects on protein aggregation state, since the effects of lipid fluidity on Ca-ATPase function are well-known. Higher temperature leads to a more fluid lipid environment, which allows faster rotational motion of the protein in the lipid membrane, which correlates with greater Ca-ATPase activity (Bigelow et al., 1986). In fact, above 20 °C, the activation energies for Ca-ATPase activity, lipid fluidity, and protein rotational motion are essentially equal (Squier et al., 1988b).

Lipid fluidity alone was once thought to explain the temperature-dependent activation of the Ca-ATPase (Hidalgo et al., 1976). However, lipid fluidity alone does not correlate well with Ca-ATPase activity under all conditions (East et al., 1984). In addition, the Arrhenius plot of Ca-ATPase activity has a change in slope at approximately 20 °C, which is inconsistent with the fluidity theory, because no such break is present in the observed fluidity increase between 4 and 40 °C (Bigelow et al., 1986). In contrast, the aggregation state of the Ca-ATPase does exhibit a striking change over this temperature range. Birmachu and Thomas (1990) found that as temperature increased from 4 to 20 °C, the relative amplitudes of two populations of smaller rotating units dramatically increased at the expense of a population of larger aggregates; whereas between 20 and 40 °C, the population of larger aggregates remained essentially unchanged, the population of middle-sized aggregates decreased slightly, and the population of the smallest rotating unit increased slightly (Birmachu & Thomas, 1990). Birmachu and Thomas (1990) interpreted the three populations, represented by the amplitudes A_1, A_2, and A_3, to be monomers, dimers, and larger aggregates (most likely tetramers) of the Ca-ATPase. There is no direct evidence that these three populations are in fact homogeneous, that is, that the A_i component of the anisotropy decay is contributed to by only monomer, dimer, or larger

aggregates of enzyme. Nevertheless, even if the three amplitudes do not represent homogeneous populations, it is clear that as temperature is increased, the equilibrium changes from a state dominated by larger aggregates at 4 °C to a state dominated by smaller aggregates by 20 °C, and finally to a state dominated by the smallest rotating units at 40 °C.

Other studies have correlated Ca-ATPase aggregation state with enzymatic activity. In one study in which melittin was used to aggregate the enzyme, the extent of aggregation correlated better with the inhibition of the enzyme than did changes in SR lipid fluidity or other physical parameters (Mahaney & Thomas, 1991; Voss et al., 1991). In another study, ether was shown to promote the formation of smaller aggregates of the Ca-ATPase from larger ones, and this action correlated well with an increase in activity (Birmachu & Thomas, 1990).

The observation that the change in the equilibrium between larger and smaller aggregates occurs at approximately the same temperature as the break in the Arrhenius plot of Ca-ATPase activity (Birmachu & Thomas, 1990) provides insight into the physical mechanism of Ca-ATPase activation by temperature. However, this observation leaves two plausible mechanisms for how Ca-ATPase aggregation state and SR lipid fluidity affect enzymatic activity between 4 and 40 °C. One explanation for the break in the Arrhenius plot is that at low temperatures larger aggregates are breaking up into dimers and monomers, both of which have greater activity than larger aggregates. Above approximately 20 °C, the primary effect of increasing temperature is to form monomers, which further increases the activity of the Ca-ATPase. An alternative explanation is that at low temperatures a dramatic increase in enzymatic activity accompanies the formation of monomers and dimers; and at higher temperatures, the increase in lipid fluidity results in more active dimers and monomers, with the formation of an additional number of monomers not affecting the activity of the enzyme.

Effect of Halothane on SR Protein Mobility. To distinguish between these two possible mechanisms, we studied the effects of halothane on lipid fluidity and protein aggregation state. EPR studies on SR lipid, and the analysis of the Ca-ATPase rotational correlation times from TPA, demonstrated that adding halothane to SR had the same effect on SR lipid fluidity (Figure 2) and protein rotational rates (Figure 4) as an increase in temperature. It has been shown previously that an increase in temperature increases the rate of rotational motion of the Ca-ATPase ($1/\phi$, eq 1) primarily by increasing the lipid fluidity (T/η, eq 1) (Birmachu & Thomas, 1990). Thus, we can now understand the mechanism of increased rotational rates observed upon the addition of halothane. Halothane increases the rate of rotational motion of the Ca-ATPase by increasing SR lipid fluidity, in agreement with the Saffman–Delbrück equation (eq 1), which states that rotational rate is proportional to lipid fluidity. Because increased lipid fluidity correlates with increased enzymatic activity in the temperature range investigated (Bigelow et al., 1986), halothane's effect on lipid fluidity should result in enzyme activation at both 4 and 25 °C.

The effect of halothane on protein aggregation state, while similar to the effect of increasing temperature, did exhibit some noticeable differences. Halothane strongly increased the population of the smallest aggregates, as shown by the 8 °C effective temperature change in A_1 at both low and high temperatures. A_2, on the other hand, changed little with the addition of halothane at 4 or 25 °C. A_3 demonstrated a 4 °C effective temperature change at low temperature and a smaller

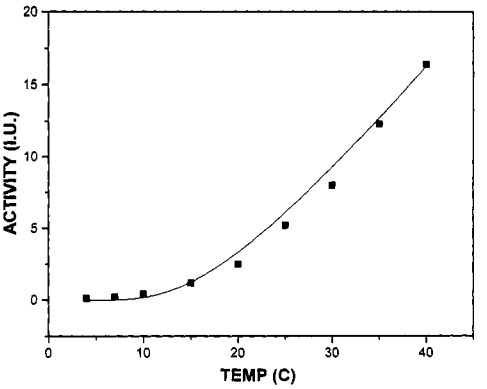

FIGURE 9: Experimental and simulated Ca-ATPase activity, showing Ca-ATPase activity between 4 and 40 °C. Each experimental data point, represented by the solid squares (■), is the average of three activity experiments, in units of micromoles of ATP hydrolyzed per milligram of protein per minute (IU), performed in the presence of 1 μg/mL of the ionophore, A23187, as measured by an enzyme-linked assay, continuous ATPase assay, described under Materials and Methods. The line is a simulation of Ca-ATPase activity, based on data obtained by EPR and TPA experiments on the changes in SR lipid fluidity and Ca-ATPase aggregation state between 4 and 40 °C (eq 2), as described in the text.

change at higher temperature. These results indicate that halothane promotes the formation of smaller rotating units, especially monomers, from larger aggregates. At low temperatures, halothane breaks up larger aggregates into dimers, and dimers into monomers, increasing the activity of the Ca-ATPase dramatically as the equilibrium shifts toward monomers and dimers as opposed to larger aggregates. At higher temperatures, the population of larger aggregates is nearly deleted, and halothane shifts the equilibrium from monomers and dimers toward a state dominated by monomers. Since halothane's effect on SR lipid fluidity should result in enzyme activation at all temperatures tested, the inhibitory effect of halothane (at higher levels of halothane and high temperature) is most likely due to the formation of monomers from dimers.

Simulation of Ca-ATPase Activity between 4 and 40 °C. We have previously discussed two possibilities for how SR lipid fluidity and Ca-ATPase aggregation state affect enzymatic activity between 4 and 40 °C. The central issue is whether the formation of monomers from dimers results in increased enzymatic activity. This does not seem likely because our results suggest that halothane inhibits enzyme activity by promoting the formation of monomers from dimers. Thus, we can now conclude that changes in aggregation state dominate Ca-ATPase activity (in the absence of halothane) at low temperature, and lipid fluidity dominates enzyme activity at higher temperatures. Using this assumption, and information obtained previously (Birmachu & Thomas, 1990) about the temperature-dependent changes in Ca-ATPase aggregation state, as well as the current data from EPR experiments describing the temperature-dependent increase in SR lipid fluidity, it should now be possible to simulate the temperature-dependent activation of control SR. Figure 9 is a plot of Ca-ATPase activity between 4 and 40 °C, measured by an enzyme-linked assay, compared to a simulation of Ca-ATPase activity based on the formula

$$\text{activity} = [\alpha \text{Flu}(T)][e^{-Y/T}][X_1(T)I_1 + X_2(T)I_2 + X_3(T)I_3] \quad (2)$$

where α is the ratio between Ca–ATPase activity and SR lipid fluidity, Flu(T) is the temperature-dependent fluidity of SR lipid determined from EPR experiments, and $e^{-Y/T}$ represents the temperature-dependent activation of the Ca-

ATPase not due to fluidity. $X_i(T)$ are the temperature-dependent mole fractions of Ca-ATPase aggregates, determined from amplitudes derived from TPA experiments performed previously by Birmachu and Thomas (1990), where $X_i = A_i/(A_1 + A_2 + A_3)$. I_i represents the intrinsic activity of putative monomers (I_1), dimers (I_2), and larger aggregates (I_3). Thus, the model predicts that enzymatic activity between 4 and 40 °C is proportional to the SR lipid fluidity, multiplied by expressions that describe the mole fractions and intrinsic activities of Ca-ATPase oligomers, and the fluidity-independent effect of temperature on enzyme activity.

To fit the experimental data, Flu(T) and $X_i(T)$ were determined from the data as described previously, and α, Y, and I_i were allowed to vary to find the best fit, using a least-squares minimization based on the Marquardt algorithm, with the additional constraint that $\sum I_i = 1$. The data were best fit by the following parameters (eq 2):

$$\alpha = 170,\ Y = 58,\ I_1 = 0.40 \pm 0.05,\ I_2 = 0.50 \pm 0.05,\ I_3 = 0.10 \pm 0.05$$

Thus, using information about the SR lipid fluidity and Ca-ATPase aggregation state, it is possible to simulate the temperature dependence of Ca-ATPase enzymatic activity. The parameters that best fit the model indicate that dimers have the greatest intrinsic activity ($I_2 = 0.50$), with monomers being slightly less active ($I_1 = 0.40$) and larger aggregates having little activity ($I_3 = 0.10$). The model predicts that shifting the equilibrium of aggregates toward monomers and dimers, which occurs when the temperature of control SR is raised from 4 to 20 °C or halothane is added at low temperature, should result in a dramatic activation of the enzyme. Increasing the temperature of control SR from 20 to 40 °C activates the ATPase, but not to the extent observed at lower temperatures, because the aggregation state changes are small in this temperature range, so lipid fluidity now dominates enzyme activation. Adding halothane at higher temperatures first activates and then inhibits enzyme function. This can also be understood in terms of the model. A halothane-dependent increase in lipid fluidity should increase the activity of the Ca-ATPase, up to the point where too many monomers are being formed at the expense of dimers. At higher concentrations of halothane, the shift in aggregation state toward monomers should inhibit enzyme function, because dimers have greater intrinsic activity than monomers. These findings are consistent with other studies that have suggested that dynamic transitions between monomers and dimers may be important for enzyme function (Napier et al., 1987a,b; Squier et al., 1988a; Kalabokis et al., 1991). If this is the case, then the mechanism of halothane inhibition of the Ca-ATPase (at higher temperatures) is depletion of the dimer state, decreasing the frequency of essential transitions between monomer and dimer forms.

Physical Mechanism of Protein Aggregation. While the effects of temperature and halothane on bilayer fluidity and protein rotational mobility can be explained by the Saffman–Delbrück equation (eq 1), the physical mechanism of protein aggregation cannot. There is no theoretical reason why changing the fluidity of the lipid environment of the SR should result in association or dissociation of proteins. Indeed, the effects of perturbants on bilayer fluidity and protein aggregation state need not be identical, as we have shown in the case of halothane. Therefore, the identification of a physical parameter that correlates exclusively with aggregation state would be invaluable in explaining the physical mechanism of the aggregation effect. Furthermore, because the addition of halothane to SR results in a relatively greater (compared to the effect of temperature) change in Ca-ATPase aggregation state than SR lipid fluidity (and fluidity changes alone cannot account for the actions of general anesthetics), it is possible that the physical mechanism that governs the Ca-ATPase aggregation state may play a key role in the mechanism of anesthesia. Several studies of SR membrane perturbants, such as ether, melittin, and alcohols, have indicated that boundary lipid properties may be affected by perturbants in a manner distinct from bulk phase lipids (Bigelow & Thomas, 1987; Lopes & Louro, 1991; Mahaney et al., 1992). In addition, temperature alone is known to change boundary lipid properties (Mahaney et al., 1992). Further investigation is needed to determine whether boundary lipid properties correlate exclusively with the changes in protein aggregation state produced by halothane.

Conclusion. The effect of temperature on Ca-ATPase activity in SR can be understood by considering the effects of temperature on SR membrane fluidity and Ca-ATPase aggregation separately. At 4 °C, the dominant aggregate population consists of larger aggregates of the enzyme, and increasing temperature has the effect of fluidizing the SR membrane and shifting the equilibrium of aggregates toward monomers and dimers. The net result is a steep increase in activity. At higher temperatures, the equilibrium is shifted toward dimers and monomers, and the rate of activation is slower as the gradual increase in membrane fluidity is responsible for enzyme activation. These two effects, the effect of aggregation at low temperatures and membrane fluidity at high temperatures, provide an explanation for the break in the Arrhenius plot of Ca-ATPase activity seen at approximately 20 °C. Consistent with these observations, halothane activates the Ca-ATPase at low temperatures by promoting a shift in the equilibrium of aggregates toward monomers and dimers, while at higher temperature halothane activates the enzyme by increasing the fluidity of the SR membrane.

ACKNOWLEDGMENT

We thank James Mahaney for critically reading the manuscript, Howard Kutchai, Razvan Cornea, John Voss, and Joe Mersol for helpful discussions, and Robert L. H. Bennett and Franz Nisswandt for technical assistance.

REFERENCES

Akeson, A., & Deamer, D. W. (1991) in *Advances in Membrane Fluidity* (Aloia, R. C., Curtain, C. C., & Gordon, L. M., Eds.) Vol. 5, pp 71–89, Wiley-Liss, New York.

Bigelow, D. J., & Thomas, D. D. (1987) *J. Biol. Chem. 262*, 13449–13456.

Bigelow, D. J., Squier, T. C., & Thomas, D. D. (1986) *Biochemistry 25*, 194–202.

Birmachu, W., & Thomas, D. D. (1990) *Biochemistry 29*, 3904–3914.

Birmachu, W., Nisswandt, F. L., & Thomas, D. D. (1989) *Biochemistry 28*, 3940–3947.

Blanck, T. J. J., Peterson, C. V., Baroody, B., Tegazzin, V., & Lou, J. (1992) *Anesthesiology 76*, 813–821.

Diamond, E. M., & Berman, M. C. (1980) *Biochem. Pharmacol. 29*, 375–381.

Eads, T. M., Thomas, D. D., & Austin, R. H. (1984) *J. Mol. Biol. 179*, 55–81.

East, J. M., Jones, O. T., Simmonds, A. C., & Lee, A. G. (1984) *J. Biol. Chem. 259*, 8070–8071.

Eckenhoff, R. G., & Shuman, H. (1991) *Ann. N. Y. Acad. Sci. 625*, 755–756.

Fernandez, J. L., Rosemblatt, M., & Hidalgo, C. (1980) *Biochim. Biophys. Acta 599*, 552–568.

Folch, J., Lees, M., & Sloane-Stanley, G. H. (1957) *J. Biol. Chem. 226*, 497–509.
Franks, N. P., & Lieb, W. R. (1991) *Science 254*, 427–430.
Gaffney, B. J. (1976) in *Spin Labeling Theory and Practice* (Berliner, L. G., Ed.) pp 567–571, Academic Press, New York.
Hidalgo, C., Ikemoto, N., & Gergely, J. (1976) *J. Biol. Chem. 251*, 4224–4232.
Kalabokis, V. N., Bozzola, J. J., Castellini, L., & Hardwicke, P. M. D. (1991) *J. Biol. Chem. 266*, 22044–22050.
Lopes, C. M. B., & Louro, S. R. W. (1991) *Biochim. Biophys. Acta 1070*, 467–473.
Louis, C. F., Zaulkernan, K., Roghair, T., & Mickelson, J. R. (1992) *Anesthesiology 77*, 114–125.
Ludescher, R. D., & Thomas, D. D. (1988) *Biochemistry 27*, 3343–3351.
Mahaney, J. E., & Thomas, D. D. (1991) *Biochemistry 30*, 7171–7180.
Mahaney, J. E., Kleinschmidt, J., Marsh, D., & Thomas, D. D. (1992) *Biophys. J.* (in press).
Napier, R. M., East, J. M., & Lee, A. G. (1987a) *Biochim. Biophys. Acta 903*, 365–373.
Napier, R. M., East, J. M., & Lee, A. G. (1987b) *Biochim. Biophys. Acta 903*, 374–380.
Nelson, T. E., & Sweo, T. (1988) *Anesthesiology 69*, 571–577.
Rock, E., Mammar, M. S., Thomas, M. A., Viret, J., & Vignon, X. (1990) *Biochimie 72*, 245–250.
Saffman, P. J., & Delbrück, M. (1975) *Proc. Natl. Acad. Sci. U.S.A. 72*, 3111–3113.
Squier, T. C., & Thomas, D. D. (1989) *Biophys. J. 56*, 735–748.
Squier, T. C., Hughes, S. E., & Thomas, D. D. (1988a) *J. Biol. Chem. 263*, 9162–9170.
Squier, T. C., Bigelow, D. J., & Thomas, D. D. (1988b) *J. Biol. Chem. 263*, 9178–9186.
Taraschi, T. F., Lee, Y. C., Janes, N., & Rubin, E. (1991) *Ann. N. Y. Acad. Sci. 625*, 698–706.
Trudell, J. R. (1991) in *Advances in Membrane Fluidity* (Aloia, R. C., Curtain, C. C., & Gordon, L. M., Eds.) Vol. 5, pp 1–14, Wiley-Liss, New York.
Voss, J., Hussey, D., Birmachu, W., & Thomas, D. D. (1991) *Biochemistry 30*, 7498–7506.
Watts, A. (1991) *Ann. N. Y. Acad. Sci. 625*, 653–667.